CONJUGATED HEAT TRANSFER ANALYSIS OF HEATED PITOT TUBES: WIND TUNNEL EXPERIMENTS, INFRARED THERMOGRAPHYAND LUMPED-DIFFERENTIAL MODELING

José Roberto Brito de Souza, jr.bs1959@gmail.com
José Luiz Zontin*, jlzzotin@gmail.com
Juliana Braga Loureiro*, jbrloureiro@gmail.com
Carolina Palma Naveira-Cotta, cpncotta@hotmail.com
Átila Pantaleão Silva Freire, atila@mecanica.ufrj.br**
Renato Machado Cotta, renatocotta@hotmail.com

Laboratory of Transmission and Technology of Heat, LTTC, Mechanical Engineering Program - PEM/COPPE/UFRJ, Centro de Tecnologia, Ilha do Fundão, Rio de Janeiro, RJ
(*)Fluid Mechanics and Anemometry Division (DINAM) – National Institute of Metrology, Standardization and Industrial Quality, INMETRO, Xerém, RJ
(**)Laboratory of Turbulence Mechanics, LMTurb, Mechanical Engineering Program - PEM/COPPE/UFRJ, Centro de Tecnologia, Ilha do Fundão, Rio de Janeiro, RJ

Abstract. *The purpose of this work is to study both theoretically and experimentally the conjugated heat transfer problem associated with the transient thermal behavior of a heated aeronautical pitot tube in a wind tunnel. The aim is to demonstrate the importance of accounting for the conduction-convection conjugation in more complex models that attempt to predict the icing of such sensors under critical atmospheric conditions. The experimental analysis involved the use of a PIV system to identify the velocity field around the selected Pitot probe for a few chosen free stream velocities, and the use of an infrared thermography system to measure the temperature field at the probe surface for different applied heating power. The theoretical analysis involves the proposition of a lumped-differential model for heat conduction which concentrates in the radial direction of the probe and maintains the local formulation along its length, where the most relevant temperature variations occur. The model is then fed with well established correlations for the heat transfer coefficients along the Pitot tube and critically compared against the experimental results for the probe surface temperatures. An excellent agreement is achieved at both steady and transient states, once the thermal capacitance of the porcelain heater insulation inside the Pitot tube body is accounted for, which plays a major role within the transient period.*

Keywords: *conjugated problem, heat transfer, infrared thermography, PIV, pitot tube, wind tunnel*

1. INTRODUCTION

Aircraft icing has been found to be a considerably negative effect on the aircraft flight performance. Ice may occur on wings, control surfaces, horizontal and vertical stabilizers, fuselage nose, landing gear doors, engine intakes, Pitot tubes, and other sensors and drain system outputs (Caliskan et al., 2008). For instance, icing of the Pitot tube reduces ram air pressure on the airspeed indicator and renders the instrument unreliable. Furthermore, this phenomenon has resulted in several incidents and fatal accidents, such as the recent tragedy with the AF447 flight. While the literature is quite rich in terms of icing and de-icing of wings and engine intakes, reporting a few different and well-known computer codes such as the classic LEWICE, ONERA2D and TRAJICE2 for icing of airfoils (Stefanini et al., 2008), only qualitative information has been published in terms of ice accretion over aircraft Pitot probes.

Aircraft icing is a very complex phenomenon that occurs during flights in clouds at temperatures at or below freezing when super-cooled water droplets impinge and freeze on the unprotected areas on which they impact (Sheriff et al., 1997). The rate and amount of ice accretion on an unheated surface depends on the shape, including surface finishing, the size, the speed at which the body is travelling, and the temperature, liquid water concentration (LWC) and the size of the droplets in the cloud (Gent et al., 2000; Myers et al., 2002; Fortin et al., 2006). While most models for airfoils icing are able to incorporate somehow all these effects towards identifying a steady-state ice accretion configuration, the research on anti-icing transient models of heated structures is much less advanced (Gent et al., 2000; Silva et al., 2007a; Silva et al., 2007b). In addition, none of the available propositions seem to incorporate a full conjugated heat transfer model that includes in detail the participating structure and heating system.

The present work is thus aimed at demonstrating the importance of accounting for conjugated conduction-convection in the transient analysis of heated Pitot tubes. For this purpose, a lumped-differential model is developed to predict temperature distributions on a Pitot probe that is internally heated through an electrical resistance, within a wind tunnel at different free stream velocities. The proposed model is radially lumped, accounting for the geometric variations along the Pitot tube length, as well as for the different materials that play a role in the heat transfer process, while the local differential formulation is maintained in the longitudinal direction, so as to allow for the determination

of the marked temperature variations along the probe body. Appropriate heat transfer coefficients correlations are employed to complete the model, for the different geometric shapes of the probe components. In order to verify the proposed model, a commercial Pitot tube that flies on the Brazilian Navy aircrafts (A4 Skyhawk), made by Aero-Instruments Co., model PH510, has been installed in a wind tunnel at the Fluid Mechanics and Anemometry Division (DINAM), National Institute of Metrology, Standardization and Industrial Quality - INMETRO, and evaluated both on the fluid mechanics and heat transfer aspects. A PIV system by DANTEC DYNAMICS is employed to analyze the flow field around the Pitot tube, while an infrared camera FLIR SC-660 is used to provide the temperature distributions at the Pitot tube surface along the experimental runs. Two free stream velocities are adjusted in the wind tunnel, for each heating power set in the Pitot tube heater, providing a few different test cases for the critical comparison of theoretical and experimental results.

2. PHYSICAL AND MATHEMATICAL MODELS

The Pitot probe employed was model PH510 by Aero-Instruments, Co., manufactured according to the standard American Armed Forces - AN 5812 - Air Force-Navy Aeronautical Standard, and employed in the A4 Skyhawk aircraft, which was gently provide by the Brazilian Navy First Aircraft Squadron of Interception and Attack. Figure 1 shows the Pitot tube, already partially painted in graphite ink for the thermographic analysis, as well as mounted on a PVC basis within the wind tunnel. The heater is embodied within the central portion of the cylindrical body of the probe and has a nominal 41 Ohm electrical resistance, with a porcelain electrical insulator.

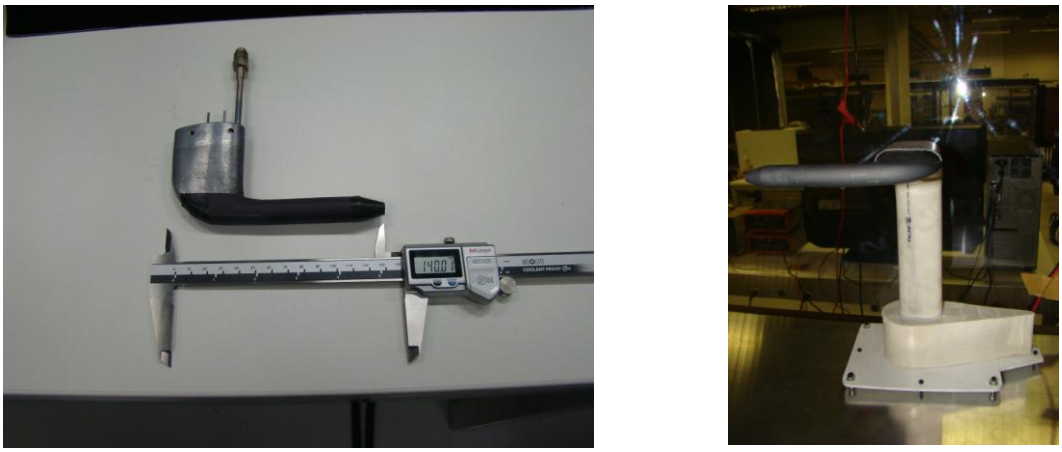

Figures 1. Pitot tube model PH 510, manufactured by Aero-Instruments, Co.

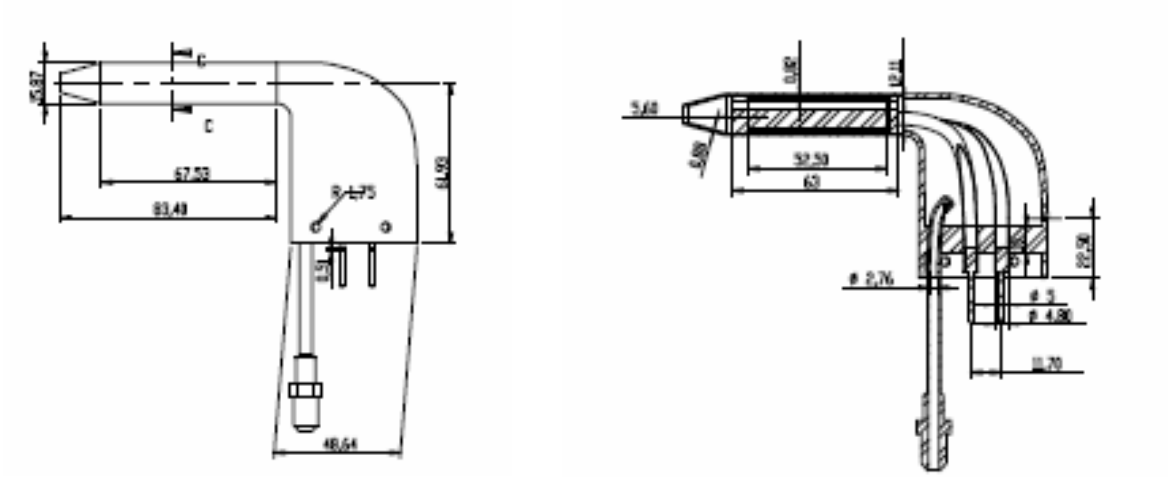

Figure 2. Dimensions of the tested Pitot tube.

The aim is to simulate the conjugated heat transfer between the heated pitot and the flow of dry air inside the wind tunnel. The free stream velocities imposed were 10 and 20 m/s at 22 ºC. The proposed conduction model consists of a partially lumped formulation, with concentration of parameters in the radial direction and local differential formulation along the probe length, neglecting the curvature at the handle of the tube, due to the lack of interest on an accurate solution at this base. The cylindrical portion of the probe is made of copper and the base profile is made of brass. The problem formulation for the radially averaged temperature distribution, $T(x,t)$, is given by:

$$\rho c_{p,ef}(x)\frac{\partial T_{av}(x,t)}{\partial t} = \frac{1}{A(x)}\frac{\partial}{\partial x}\left[k_{ef}(x)A(x)\frac{\partial T_{av}(x,t)}{\partial x}\right] - h(x)\frac{p(x)}{A(x)}\,T_{av}(x) - T_{\infty} + g_{av}(x,t),\ 0 < x < L,\ t > 0 \tag{1}$$

with initial condition and boundary conditions given by:

$$T_{av}(x,0) = T_0(x),\quad 0 < x < L \tag{2}$$

$$-k_{ef}(0)\left.\frac{\partial T_{av}(x,t)}{\partial x}\right|_{x=0} = h_e[T_{\infty} - T_{av}(0,t)],\quad t > 0 \qquad \left.\frac{\partial T_{av}(x,t)}{\partial x}\right|_{x=L} = 0,\quad t > 0 \tag{3,4}$$

where the variables shown above correspond to ρ, density [kg/m^3], c_p, specific heat [J/(kg ºC)], ef stands for effective property, T_{av}, transversally averaged temperature [ºC], x, longitudinal coordinate [m], k_{ef}, thermal conductivity [W/(m ºC)], A, cross-sectional area [m^2], p, cross-section perimeter [m], h, heat transfer coefficient [W/(m^2 ºC)], t, time [s], T_{∞}, temperature outside boundary layer [ºC], g_{av} (x,t), transversally averaged energy generation density [W/m^3], h_e, heat transfer coefficient at stagnation region [W/(m^2 ºC)], T_0(x), initial temperature distribution, [ºC].

Figures 3 show the functions of the x coordinate utilized in the model for the parameters and thermophysical properties, as a result of the geometric and materials variations within the probe body. For instance, the tip of the Pitot tube has a conical section, which together with most of the cylindrical portion is made of copper, until a soldered joint switches the material to brass, then following the wing shaped base. In addition, the heater and the porcelain insulator can be found only at the central portion of the cylindrical copper tube. Also, appropriate correlations are obtained from the literature to estimate the heat transfer coefficients at the different regions, stagnation region, cone and cylindrical bodies, and wing shaped base (Sparrow et al., 2004; Tong & Hu, 2009).

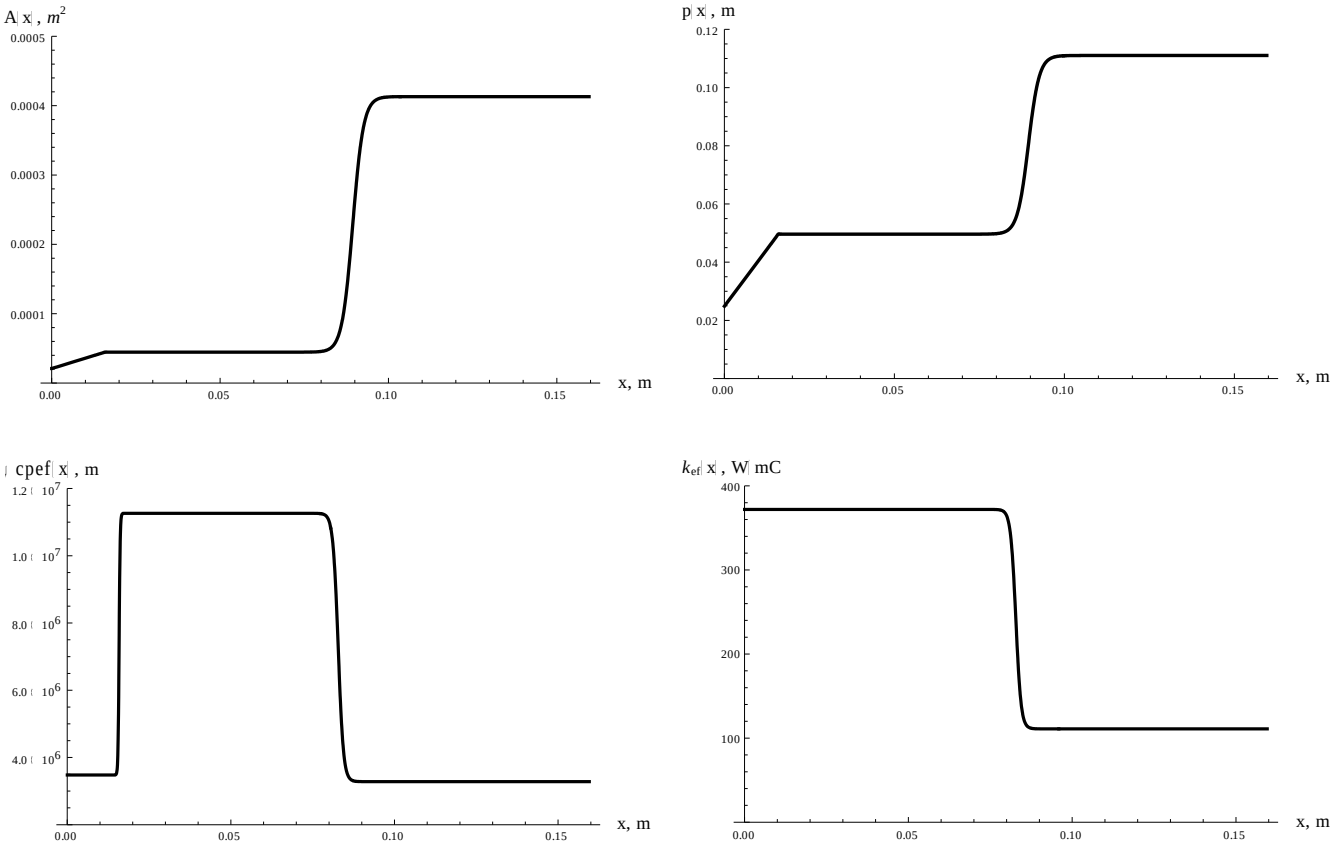

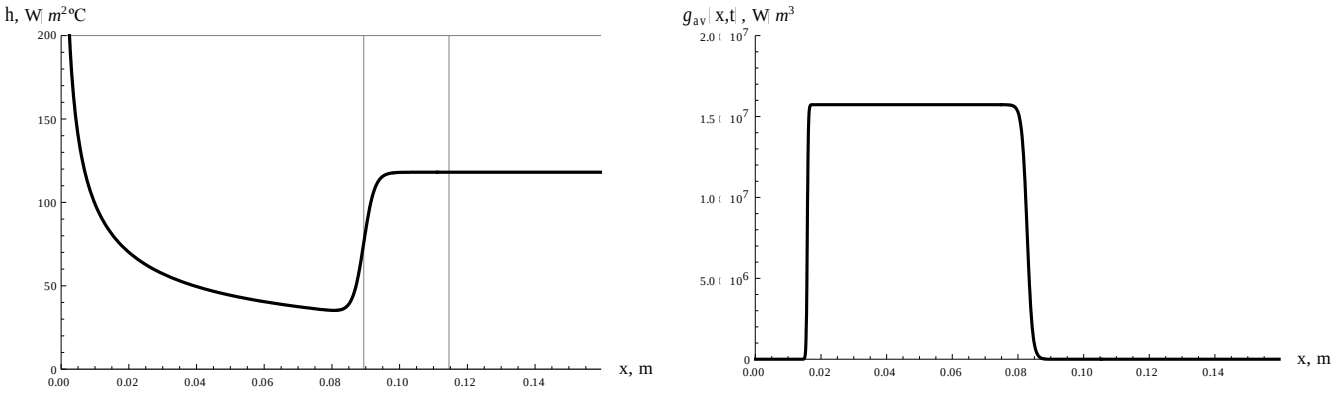

Figures 3. Longitudinal variation of parameters and effective thermophysical properties employed in the model.

The proposed model of Eqs.(1-4), together with the identified parameters and properties depicted in Figures 3, were implemented in the symbolic-numerical platform *Mathematica* v.7.0 (Wolfram, 2005), and numerically solved through the Method of Lines available in the subroutine NDSolve. The numerical results were also verified against the error controlled solution in the UNIT code (Unified Integral Transforms) (Sphaier et al., 2009; Cotta et al., 2010), which implements an automatic hybrid numerical-analytical solution based on the Generalized Integral Transform Technique (GITT) (Cotta, 1993; Cotta & Mikhailov, 1997; Cotta & Mikhailov, 2006).

3. APPARATUS AND EXPERIMENTAL PROCEDURE

The experimental results of the heated Pitot tube presented in this work were obtained in an aerodynamic wind tunnel at the Fluid Mechanics and Anemometry Division (DINAM), in the National Institute of Metrology, Standardization and Industrial Quality - INMETRO, and is shown in Figure 4 below. It is an open circuit blower type tunnel and consists of a test section of 500 mm x 500 mm, 8 m long, and a 12.5 HP fan with variable speed control from 0 to 23 m/s. The main components of this experimental setup are the infrared camera FLIR SC660, a high performance infrared system with 640x480 image resolution used to obtained the temperature field at the Pitot surface and the Particle Image Velocimetry (PIV) system, laser and camera, by DANTEC DYNAMICS with a pulse duration of nano seconds, wavelength of 1064 and 532nm with a laser medium of Nd:YAG. Other components of the setup are: (a) an anemometer (FCO510) by MICROMANOMETER and a reference tunnel pitot by DWYER; (b) a source of alternate power (Variac), with capacity of up to 100 V; (c) three multimeters to measure the Pitot resistance, the current and voltage applied at the Pitot resistance; (d) a microcomputer for data acquisition; (e) the Pitot`s tube support. The Pitot probe was fixed to the floor of the wind tunnel through a PVC support and in order to reduce uncertainty in the IR camera readings, its surface was painted with a graphite ink, which brought its emissivity to around $\varepsilon = 0.97$, as stated by the ink manufacturer.

Figure 4. Open circuit blower type wind tunnel of DINAM-INMETRO.

The experimental procedure is initiated by imposing a velocity to the wind tunnel test section, followed by the application of a voltage difference to the Pitot´s electrical resistance. Voltage and current are simultaneously measured along the experiment. Due to space limitations, the infrared thermography camera and laser source of the particle image velocimetry are not installed simultaneously, since both were required to be placed perpendicularly to the Pitot tube. Therefore, first the infrared thermography measurements are taken along the transient process up to steady-state, and then the PIV measurements are performed. Figure 5a shows the installation of the infrared câmera at the top of the wind tunnel test section, and its positioning with respect to the Pitot tube, while Figure 5b shows the laser source installation in place of the IR câmera, for the second phase of the experiment.

Figure 5a. Detail of the IR câmera installation

Figure 5b. Detail of the PIV laser positioning

For the IR images acquisition the camera is connected to the acquisition computer by a fire-wire cable that makes it possible fast transference of acquired data. Using the FLIR´s proprietary software called "ThermaCam Reseacher 2.9" one can remotely operate the thermography camera, and monitor the temperature increase. Figures 6 illustrate the IR image produced by the FLIR SC660 camera of the heated Pitot tube in the beginning of the transient regime (Fig. 6a) and after the steady-state is achieved (Fig.6b). One may clearly observe the temperature rise at the region of the Pitot heater and the temperature drop throughout the Pitot wing-shaped base (note that Fig. 6a is much less brighter than Fig. 6b).

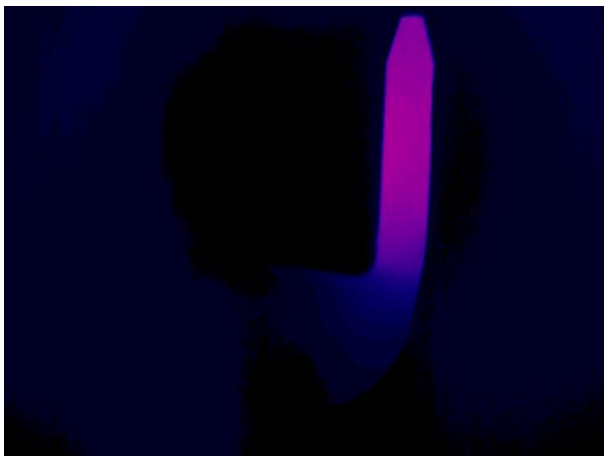

(a)

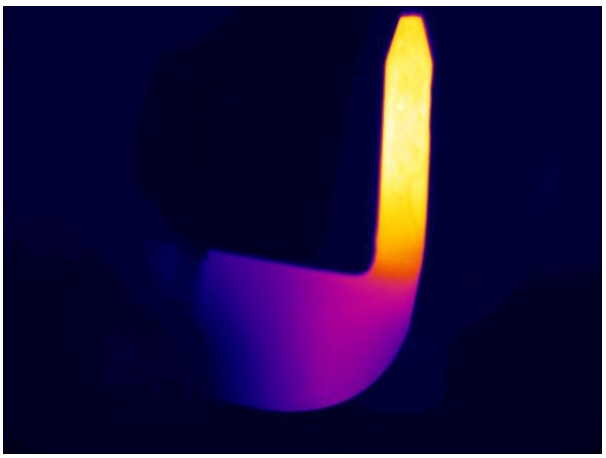

(b)

Figures 6. IR image of Pitot tube for an air flow free stream velocity of 10 m/s: a) few seconds after the heater is turned on; b) steady-state.

Once steady-state has been achieved, the IR câmera is substituted by the laser source and the second phase of the experiment is initiated. Particle Image Velocimetry is a technique for measuring fluid flow which is becoming increasingly in scientific circles because of its non-intrusive measurement characteristics (Marins et al., 2009). The region we wish to study in the 2D case is illuminated by the laser light plane. As we introduce tracer particles dispersed in the fluid, a digital camera (the image is obtained by stimulating a group of photosensitive capacitors known as CCD, charge-couple-device) installed perpendicular to the laser plan, captures images from the particles illuminated by the laser. Figure 7 shows the laser digital camera manufactured by FlowSense, used in our experiments.

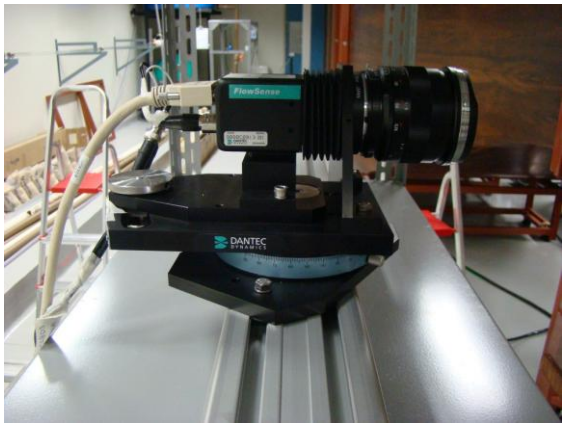

Figure 7. Detail of the PIV laser camera

In Figure 8a we can observe the Pitot tube illuminated by a constant plane of laser during the PIV test and Figure 8b illustrates a photo of the Pitot tube taken by the PIV camera. The particle used in the wind tunnel tests were obtained using a plain smoke generator (Chauvet Hurricane 1700), which uses a fluid (ROSCO) of polyvalent alcohols, essence, dye and deionized water to generate the smoke. In Figures 9 we can observe the average velocity field vector calculated by the PIV software, showing the boundary layer at the Pitot upper surface, respectively for 10 and 20 m/s dry air speed in the wind tunnel, confirming that the flow is essentially laminar over the experimental setup at such free stream velocities.

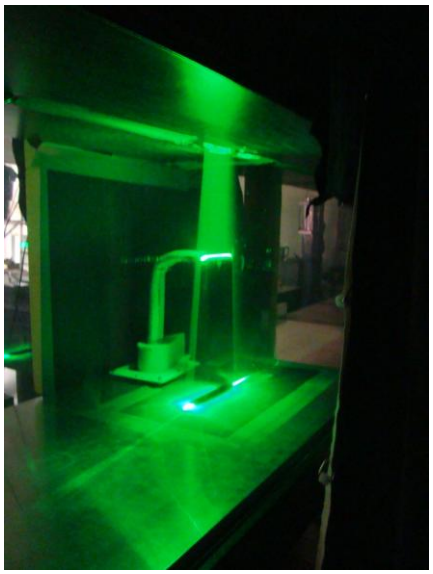

Figure 8a. Pitot tube illuminated by laser during PIV test

Figure 8b. Pitot tube photo by PIV camera

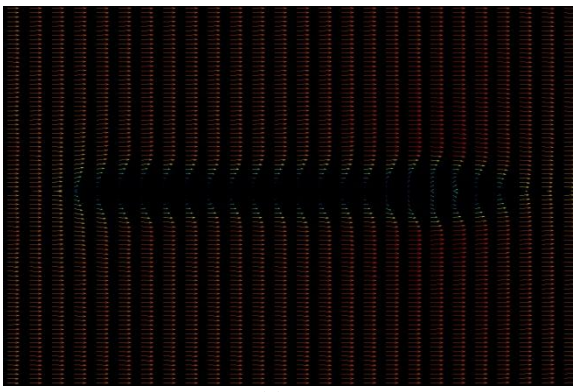

(a) 10m/s

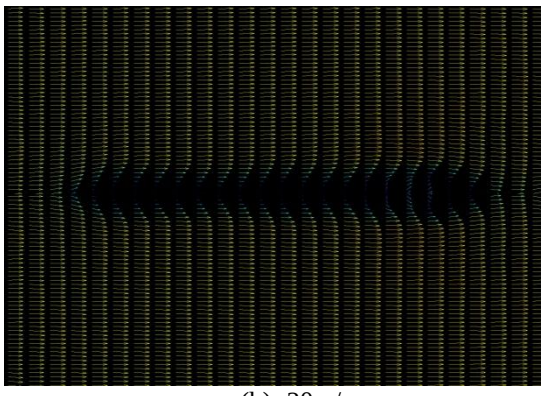

(b) 20m/s

Figures 9. Average velocity field vector over upper Pitot tube surface calculated by PIV software

4. RESULTS AND DISCUSSION

Once the thermographic images have been acquired by the IR camera, one may select points within the Pitot tube domain to form lines and analyze its transient behavior. Here, we illustrate the results obtained for two sets of points, corresponding to lines (LI01) and (LI02), as shown in Figure 10 below. LI01 is chosen along the longitudinal direction of the Pitot tube, extending to the wing-shaped base normally to the isotherms. LI02 is perpendicular to the longitudinal axis, and was used to verify that the temperature gradients are in fact negligible in this direction. Figure 11 thus presents the temperature distributions along these two lines, confirming the marked temperature drop along the longitudinal line (LI01) and the practically uniform temperatures across the tube axis (LI02).

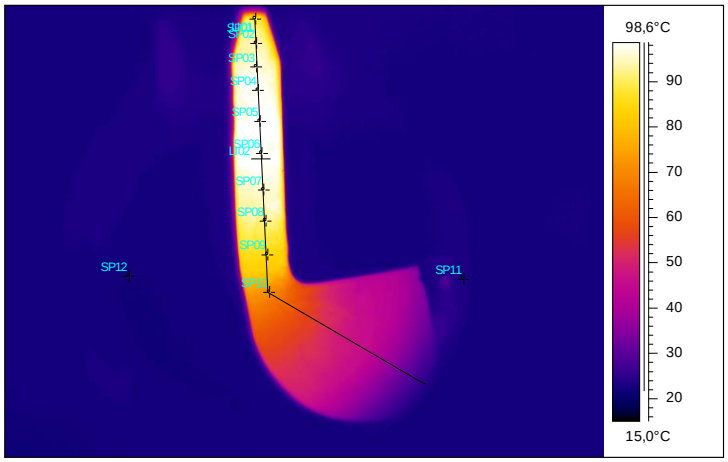

Figure 10. Example of data extraction from the thermographic images (longitudinal and transversal lines).

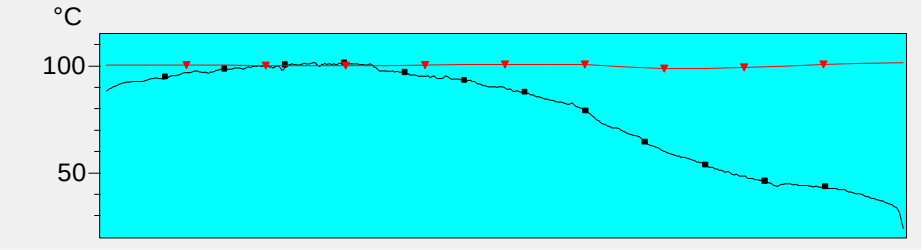

Figure 11. Temperature distributions obtained from the marked lines on the thermographic image (longitudinal line in black, transversal line in red).

A total of seven experiments were conducted in the wind tunnel, for the two freestream velocity values and also different applied voltages on the Pitot heater. Two experiments were conducted with equal input parameters, for verifying the repeatability of the experimental setup and procedure. Figure 12 illustrates the experimental surface temperatures obtained through the infrared thermography images at steady-state, for experiments no.6 and 7, which shows an excellent agreement between the two independent measurements. One may also note the higher values of temperature achieved within the heated portion of the cylinder and the progressive temperature decay as the wing section base is approached.

Figure 13 below shows the comparison of the experimental surface temperatures against the theoretical predictions, again for steady-state and along the Pitot tube length. Three vertical lines are shown that correspond, from left to right, to the end of the conical section, to the transition between copper and brass within the cylindrical region, and to the beginning of the wing-shaped base. The infrared camera measurements are shown in red, while the blue curve corresponds to the simulation with an effective heat transfer coefficient including the radiation in linearized form and the green curve is related to the simulation with the nonlinear radiation model, thus slightly modifying Eq.(1) by adding the heat losses by radiation in explicit form. One can see that both simulation results are in excellent agreement with the experimental results, and with very little difference between themselves, throughout the active body of the Pitot tube. Only after the middle of the base length one can observe significant deviations, as expected, since the model was simplified in this region not accounting for the curvature effects, in light of the irrelevance of the predictions in this region. We can also observe some slight experimental temperature fluctuations right after the cone-cylinder transition, which cannot be predicted by the proposed model.

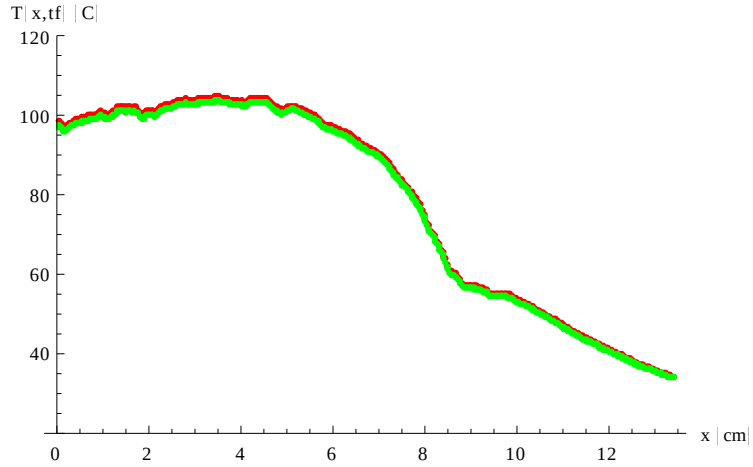

Figure 12. Experimental surface temperatures at steady-state: Repeatability of two experiments (nos.6 & 7), with 10 m/s, 68 V and 0.69 A.

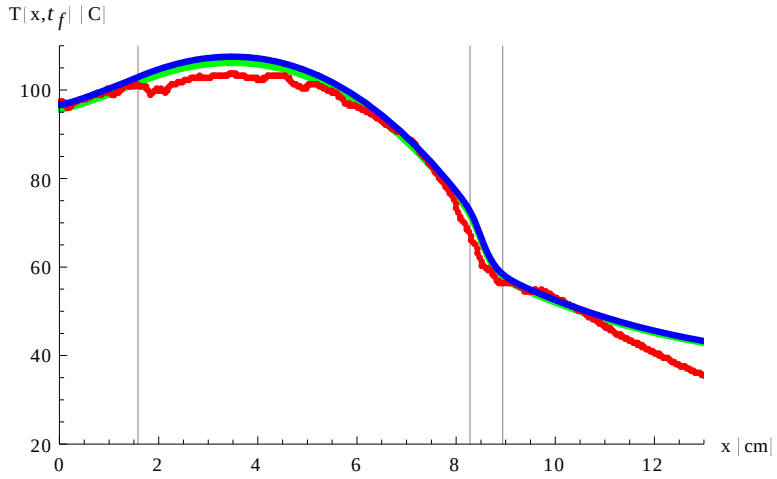

Figure 13 Comparison of experimental and simulated surface temperatures at steady-state: Experimental in red, linearized radiation in blue, nonlinear radiation in green (Exp.6, 10 m/s, 68 V and 0.69 A).

Figures 14 present the comparative transient behavior of the experimental and simulated surface temperatures at various positions along the conical and cylindrical sections of the Pitot tube. An excellent agreement is observed throughout the transient period and for all the positions shown, despite the complex configuration of the device vis-à-vis the simplicity of the proposed model. Slight deviations are observable again in the region following the cone-cylinder transition, which do not perfectly reproduce the steady-state result but follow the transient behavior of the experiment. It must be mentioned that accounting for the porcelain influence in the effective thermal capacitance at the heater region was crucial in obtaining this agreement between experiments and model, which obliged us to cut open the Pitot tube to extract the geometric details of the internals.

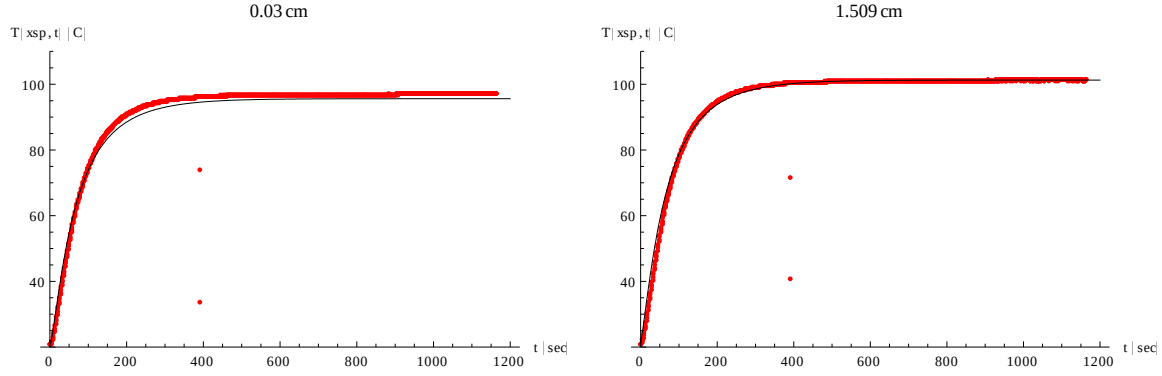

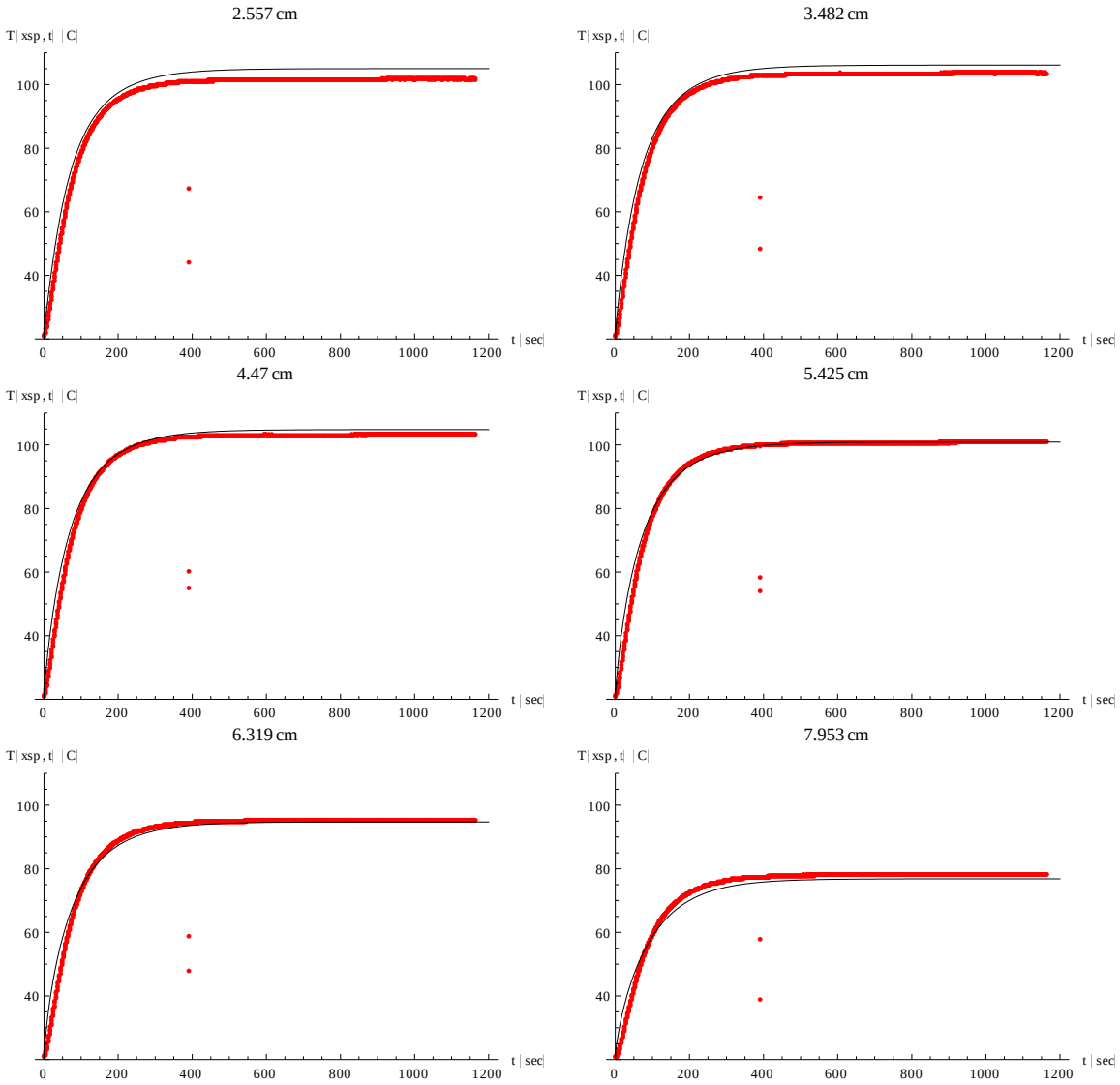

Figure 14. Transient behavior of surface temperatures at different longitudinal positions: Experimental in red, simulated in black (Exp.6, 10 m/s, 68 V and 0.69 A).

5. CONCLUSIONS

An experimental analysis of a heated Pitot tube in an aerodynamic wind tunnel is undertaken, by employing infrared thermography to raise the surface temperatures evolution and particle image velocimety to map the flow around the probe. Then, a simplified lumped-differential model is proposed to simulate the temperatures distribution along the length of the tube and with time. An excellent agreement was reached between the experimental and simulated results along the transient once the thermal capacitance of the electrical porcelain insulator of the Pitot tube heater was accounted for. This effort is aimed at demonstrating that conjugated convection-conduction heat transfer cannot be omitted when dealing with the analysis of heated Pitot tubes, even at low speeds and room temperatures for the free stream. Therefore, it should be mandatory to include the participation of the Pitot tube body in the prediction of icing and on the design of anti-icing systems for such sensors.

6. ACKNOWLEDGEMENTS

The authors are indebted to the Brazilian Navy, for providing the Pitot tubes employed in the tests. The partial financial support of INMETRO, CNPq and PRONEX-FAPERJ (Nucleo de Excelência em Turbulência) is also acknowledged. This work is dedicated to the 228 victims of the AF447 and their families, hoping that such hard lessons will affect somehow technology development in a progressively more competitive world, by strictly bounding it with scientific analysis.

7. REFERENCES

Caliskan; F., Aykan, R., and Hajiyev, C., 2008, "Aircraft Icing Detection, Identification, and Reconfigurable Control Based on Kalman Filtering and Neural Networks", J. of Aerospace Engineering, v. 21, no. 2, pp.51-60.

Cotta, R.M. , 1993, "Integral Transforms in Computational Heat and Fluid Flow", CRC Press, Boca Raton.

Cotta, R.M. and Mikhailov, M.D., 1997, "Heat Conduction: Lumped Analysis, Integral Transforms, Symbolic Computation", Wiley-Interscience, Chichester, UK.

Cotta, R.M., 1998, "The Integral Transform Method in Thermal and Fluids Sciences and Engineering", Begell House, New York.

Cotta, R.M. e Mikhailov, M.D., 2006, "Hybrid methods and symbolic computations", in: Handbook of Numerical Heat Transfer, 2nd edition, Chapter 16, Eds. W.J. Minkowycz, E.M. Sparrow, and J.Y. Murthy, John Wiley, New York.

Cotta, R. M., Quaresma, J. N. N., Sphaier, L. A., Naveira Cotta, C. P., 2010, "Unified Integral Transform Approach in the Hybrid Solution of Multidimensional Nonlinear Convection-Diffusion Problems", 14th Int. Heat Transfer Conf., Washington, DC, USA, August.

Fortin, G., Laforte, J.L., and Ilinca, A., 2006, "Heat and Mass Transfer during Ice Accretion on Aircraft Wings with an Improved Roughness Model", Int. J. Thermal Sciences, v.45, pp.595-606.

Gent, R. W., Dart, N. P., and Cansdale, J. T., 2000, "Aircraft Icing", Phil. Trans. R. Soc. Lond. A, v. 358, pp.2873-2911.

Marins, L.P.M., Duarte, D.G., Loureiro, J.B.R., Moraes, C.A.C., Silva Freire, A.P. , 2009, "LDA and PIV Characterization of the Flow in a Hydrocyclone without an Air-core", Journal of Petroleum Science & Engineering, pp. 168-176.

Myers, T.G., Charpin, J.P.F., and Thompson, C.P., 2002, "Slowly Accreting Ice due to Supercooled Water Impacting on a Cold Surface", Physics of Fluids, v.14, no.1, pp.240-256.

Sherif, S.A., Pasumarthi, N., and Bartlett, C.S., 1997, "A Semi-empirical Model for Heat Transfer and Ice Accretion on Aircraft Wings in Supercooled Clouds", Cold Regions Science and Technology, v.25, pp.165-179.

Silva, G. A. L., Silvares, O. M., and Zerbini, E. J. G. J., 2007a, "Numerical Simulation of Airfoil Thermal Anti-ice Operation. Part 1: Mathematical Modeling," Journal of Aircraft, v. 44, no. 2, pp. 627-633.

Silva, G. A. L., Silvares, O. M., and Zerbini, E. J. G. J., 2007b, "Numerical Simulation of Airfoil Thermal Anti-ice Operation. Part 2: Implementation and Results," Journal of Aircraft, v. 44, no. 2, pp. 634-641.

Sparrow, E.M., Abraham, J.P., Tong, J.C.K., 2004, "Archival Correlations for Average Heat Transfer Coefficients for Non-circular and Circular Cylinders and for Spheres in Cross-flow", Int. J. Heat & Mass Transfer, v.47, pp.5285-5296.

Sphaier, L. A., Naveira Cotta, C. P., Cotta, R. M., Quaresma, J. N. N., 2009, "The UNIT (Unified Integral Transforms) Symbolic- Numerical Computational Platform for Benchmarks in Convection-Diffusion Problems", Proceedings of the 30th CILAMCE Congresso Ibero Latino Americano de Métodos Computacionais em Engenharia (CILAMCE), 2009, Buzios, RJ, Brazil.

Stefanini, L. M., Silvares, O. M., Silva, G. A. L., and Zerbini, E. J. G. J., 2008, "Boundary-Layers Integral Analysis - Airfoil Icing," AIAA Paper 2008-0474, Aerospace Sciences Meeting and Exhibit, 46th, 2008, Reno, American Institute of Aeronautics and Astronautics, Reston, Janeiro 2008.

Tong, Z.M., and Hu, Y.H., 2009, "Convective Heat Transfer and Flow Resistance Characteristics of Various Types of Elliptical Tubes", Proc. of the Int. Conf. on Energy and Environment Technology, IEEE, 2009.

Wolfram, S., 2005, "The *Mathematica* Book", Cambridge-Wolfram Media.

8. RESPONSIBILITY NOTICE

The authors are the only responsible for the printed material included in this paper.